Full counting statistics of the momentum occupation numbers of the Tonks-Girardeau gas

P. Devillard,[1] D. Chevallier,[2] P. Vignolo,[3] and M. Albert[3]
[1]*CPT, CNRS, Aix Marseille Université, Université de Toulon, 13288 Marseille, France*
[2]*Department of Physics, University of Basel, Klingelbergstrasse 82, 4056 Basel, Switzerland*
[3]*Institut de Physique de Nice, CNRS, Université Côte d'Azur, 06108 Nice, France*

(Received 19 March 2020; accepted 18 May 2020; published 1 June 2020)

We compute the fluctuations of the number of bosons with a given momentum for the Tonks-Girardeau gas at zero temperature. We show that correlations between opposite momentum states, which are an important identifying characteristic of long-range order in weakly interacting Bose systems, are suppressed and that the full distribution of the number of bosons with nonzero momentum is exponential. The distribution of the quasicondensate is however quasi-Gaussian. The experimental relevance of our findings for recent cold-atom experiments is discussed.

DOI: 10.1103/PhysRevA.101.063604

I. INTRODUCTION

Ultracold-atom experiments represent now an established playground to test theories of many-body physics and mimic solid-state strongly correlated systems [1,2] with incredible accuracy. One-dimensional systems can be routinely achieved by confining atoms along transverse directions [3–5] with the possibility to monitor the interaction strength and the temperature at will. In particular, it is possible to span the entire range of the one-dimensional Bose gas from the weakly interacting to the strongly interacting regime. While pair correlations have a tendency to build albeit without forming a true condensate in the weak-coupling limit, strong repulsion tends to make the bosons behave more like fermions. This is the celebrated Tonks-Girardeau gas [6]. Although physical quantities involving diagonal elements of the density matrix such as spatial density correlations [3] or the real-space emptiness formation probability [7] are fermion-like, the off-diagonal part behaves very differently. The most common example is the momentum distribution, namely, the average occupation number of a state with a given momentum p, $\langle N_p \rangle$, which is the so-called Fermi-Dirac distribution for fermions but is completely different for bosons [8,9].

This momentum distribution is a key observable in the field of ultracold atoms since it is easily obtained experimentally with time-of-flight images and contains crucial information on quantum correlations, interaction effects, and symmetries of the many-body wave function [10]. However, as we know from quantum optics, mesoscopic transport or even the physics of phase transitions, the fluctuations around the average are sometimes the most interesting physical signal. This is why the community is now studying higher moments of the momentum occupation number, like its variance $\langle N_p^2 \rangle - \langle N_p \rangle^2$, covariance $\langle N_p N_q \rangle$ [11–16], or even the full distribution (full counting statistics) [15]. This can be a great help in unraveling different regimes [11,13,17,18] or in identifying exotic phenomena such as the dynamical Casimir effect [19] or Hawking radiation [20–24].

In this paper we study the fluctuations of the momentum occupation number N_p in the Tonks-Girardeau limit at zero temperature for all momenta. This is an extension of the work of Lovas *et al.* [15] on the full counting statistics of N_p in the low-momentum regime described by bosonization [25,26] and the one of Refs. [11,13,14] on the weakly interacting Bose gas. In particular, we show that the full counting statistics of N_p is, for momentum p in almost all regimes, exponential and that the different occupation numbers are uncorrelated. This is in sharp contrast to the weakly interacting regime where Bogoliubov theory predicts positive correlations between opposite momentum states [11,14,27].

This article is organized as follows. In Sec. II we describe the model and explain the general formalism used to compute the second moment $\langle N_p^2 \rangle$ and the correlations $\langle N_p N_q \rangle$ of the momentum occupation number in terms of Toeplitz matrices. Section III concentrates on intermediate- and long-wavelength properties. It explains how results from standard bosonization [15] can be retrieved. Section IV deals with the opposite limit of high momentum. A short-distance expansion of the two-body density matrix enables us to make predictions about the variance of the number of particles with a given momentum. The full probability distribution is also obtained. Sections V and VI complement our analytical results with numerical calculations of the variance and the correlations for all values of the momentum and for the specific case of the quasicondensate mode. In Sec. VII we discuss how our predictions could be tested in realistic experiments as well as perspectives for future research on other systems along these lines. Technical details can be found in Appendixes A–C.

II. MODEL

We consider a gas of N identical bosons existing on a strictly one-dimensional segment of length L with periodic boundary conditions. The average density $\rho = N/L$ is constant and we will mainly be interested in the thermodynamic limit $N \to \infty$ and $L \to \infty$ with N/L fixed. However, the formalism also allows us to straightforwardly calculate finite-size

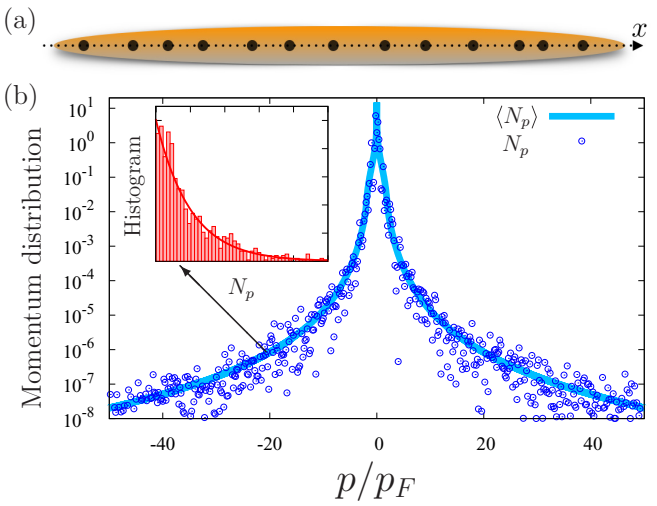

FIG. 1. (a) One-dimensional identical interacting bosons at zero temperature. (b) Sketch of the momentum distribution of the one-dimensional Bose gas in the Tonks-Girardeau limit ($p_F = \pi\hbar N/L$). The data represent a single shot measurement whereas the full line is the average $\langle N_p \rangle$. The inset shows the full distribution of N_p for a given p.

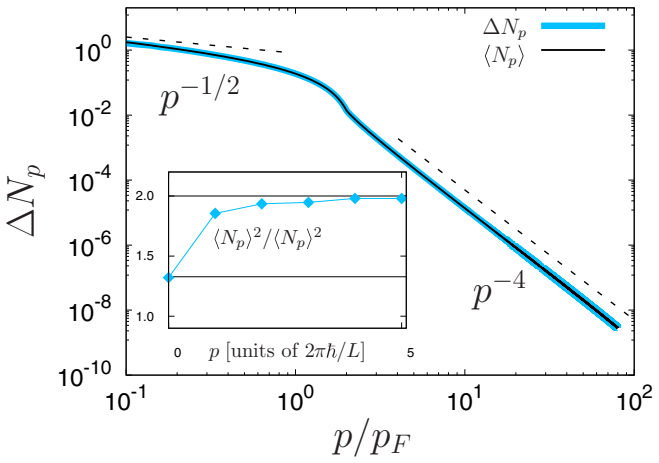

FIG. 2. Standard deviation $\Delta N_p = \sqrt{\langle N_p^2 \rangle - \langle N_p \rangle^2}$ (blue thick solid line) and average number of bosons $\langle N_p \rangle$ (black thin solid line) as a function of p for $N = 100$ bosons. Dashed lines are the limiting cases (see the text). The inset shows the same data in linear scale in a slightly different form. The ratio $\langle N_p^2 \rangle / \langle N_p \rangle^2$ is plotted as a function of the momentum p in units of $2\pi\hbar/L$. The horizontal black lines correspond to the two limiting values 1.33 and 2 [see Eqs. (19) and (10)]. The blue solid line connecting the data points is merely a guide to the eye.

corrections. We focus on the limit of infinite and hard-core repulsion between bosons, which is known as the Tonks-Girardeau gas. The Hamiltonian is a limiting case of the Lieb-Liniger model [28], which reads

$$\mathcal{H} = -\frac{\hbar^2}{2m}\sum_{i=1}^{N}\frac{\partial^2}{\partial x_i^2} + g\sum_{i>j}\delta(x_i - x_j), \tag{1}$$

where x_i is the position of the ith bosonic particle of mass m and g is the repulsive interaction strength [29]. In the Tonks limit, g is sent to infinity. In this regime, the ground state is constructed by filling all the momentum states up to the Fermi momentum $p_F = \hbar\pi N/L$ while preserving the bosonic statistics as described below. This is the so-called regime of fermionization where all physical observables that depend only on density or density correlations are similar to the ones of a perfect gas of fermions [6]. However, quantum statistics is crucial whenever off-diagonal elements of the density matrix are involved in an observable and this is in particular the case of the momentum distribution [8,9]. This quantity $\langle N_p \rangle$ is the Fourier transform of the one-body density matrix

$$\langle N_p \rangle = \iint e^{-ip(x-x')/\hbar}\rho_1(x,x')dx\,dx', \tag{2}$$

$$\rho_1(x,x') = \int \Psi^*(X)\Psi(X')dx_2\cdots dx_N, \tag{3}$$

where $X = (x, x_2, \ldots, x_N)$, $X' = (x', x_2, \ldots, x_N)$, and $\Psi(x_1, \ldots, x_N)$ is the many-body wave function of the system, which corresponds to the average number of bosons in a state with momentum p and therefore is proportional to the probability of finding a particle with momentum p in an actual experiment. For the Tonks-Girardeau gas considered in this paper, its shape is represented in Fig. 1 (thick blue line), which obviously shows that it has no relation with the one of a perfect Fermi gas (a Fermi-Dirac step function at zero temperature). Therefore, much important information is accessible from this observable such as the quasicondensate fraction or the symmetry of the wave function. In the Tonks regime, it is known to display several interesting properties. First, the average occupation of the ground state ($p = 0$ here) is proportional to $\sqrt{N}$ [8,30] and not N like in a weakly interacting Bose gas, signaling the absence of Bose-Einstein condensation in one dimension in the presence of strong interactions. At low momentum, namely, for $p \ll p_F$, the momentum distribution decays as $1/\sqrt{p}$, while for $p \gg p_F$ it decays as p^{-4}. The latter behavior is universal as long as particles have contact interactions and does not depend on quantum statistics or on the interaction strength. The coefficient in front of this power law, however, strongly depends on these parameters and is called the Tan contact [31,32]. Some of these features are illustrated in Fig. 2 (thin black solid line and black dashed lines on the main panel).

However, the momentum distribution is only an average quantity. In an experiment, shot-to-shot fluctuations (blue circles in Fig. 1) may be an incredible source of information, as it was pointed out by Landauer in his famous quote "the noise is the signal." With the important advances in the field of single-atom detection [33], fluctuations around the average will be an additional channel for collecting precious information about the physical properties of quantum liquids, but there seems to be very little information about them in the literature. For example, the variance $\langle N_p^2 \rangle - \langle N_p \rangle^2$ is not known in general. Recently, Lovas *et al.* [15] calculated the probability distribution of the momentum occupation, but only in the long-wavelength limit, using bosonization [3]. They found that N_p is distributed exponentially in this regime for $p \neq 0$ and that N_0 follows a Gumbel distribution for weak interactions. In the opposite limit of high momentum or for a strong interaction, nothing is known at the moment. It is

the purpose of this paper to answer these questions. We now explain how to compute the variance, the covariance, and the full distribution of N_p for a Tonks-Girardeau gas at zero temperature.

In order to calculate the fluctuations of N_p, we need the two-body density matrix, defined as

$$\rho_2(x,u;y,w) = \iint\cdots\int \Psi^*(x,u,x_3,\ldots,x_N) \times \Psi(y,w,x_3,\ldots,x_N)dx_3\cdots dx_N, \quad (4)$$

with Ψ the ground-state wave function for periodic boundary conditions [6]

$$\Psi(\{x_i\}) = \frac{1}{\sqrt{N!L^N}} \prod_{1\leqslant j<k\leqslant N} |e^{i(2\pi/L)x_j} - e^{i(2\pi/L)x_k}|. \quad (5)$$

Following the steps done in Ref. [30] for the one-body density matrix, we apply the method therein to the two-body density matrix and cast $\rho_2(x,u;y,w)$ as a determinant of a Toeplitz matrix. Technical details are given in Appendix A. This results in

$$\rho_2(x,u;y,w) = \frac{1}{L^2}|e^{i\theta_u} - e^{i\theta_x}||e^{i\theta_w} - e^{i\theta_y}|\det(\Gamma_{i,j}), \quad (6)$$

where $\theta_x = 2\pi x/L$ (θ_y, θ_u, and θ_w are defined in a similar fashion) and det denotes the determinant of the matrix Γ of elements $\Gamma_{i,j}$. This matrix is of Toeplitz type, which means that $\Gamma_{i,j}$ is a function of $n = i - j$ only. In addition, Γ is also Hermitian. Explicitly,

$$\Gamma_n = \int_0^{2\pi} F(\theta)e^{in\theta}\frac{d\theta}{2\pi}, \quad (7)$$

where

$$F(\theta) = 16\left|\sin\left(\frac{\theta-\theta_x}{2}\right)\sin\left(\frac{\theta-\theta_y}{2}\right) \times \sin\left(\frac{\theta-\theta_u}{2}\right)\sin\left(\frac{\theta-\theta_w}{2}\right)\right|. \quad (8)$$

Finally, the second moment $\langle N_p^2\rangle$ can be calculated by taking a double Fourier transform of $\rho_2(x,u;y,w)$. The covariance, namely, the correlations between occupation numbers at different momenta p and q, is written as

$$\langle N_pN_q\rangle = \int_{[0,L]^4} e^{i[p(y-x)/\hbar]}e^{i[q/(w-u)\hbar]} \times \rho_2(x,u;y,w)dx\,dy\,du\,dw. \quad (9)$$

Following this recipe, we will now evaluate these quantities analytically at low momentum in Sec. III and high momentum in Sec. IV and numerically in Sec. V for any momentum. The reader not interested in technical details may want to go directly to Sec. V. Finally, the quasicondensate case ($p = 0$) is treated separately in Sec. VI.

III. FLUCTUATIONS IN THE HYDRODYNAMIC REGIME

In this section we explain how to retrieve the findings of Ref. [15] on the full distribution of N_p but also compute the covariance in the low-momentum regime. Instead of standard bosonization, which is commonly used to describe the physics at low energy, we develop an alternative and more general approach based on asymptotic properties of Toeplitz matrices. At low momentum $p \ll p_F$ but $p \neq 0$, or long distances compared to $\xi = L/N$, the mean interparticle distance, we show that

$$\langle N_pN_q\rangle = (1+\delta_{p,q})\langle N_p\rangle\langle N_q\rangle. \quad (10)$$

To do so, we first compute the two-body density matrix in the limit of low momentum as explained in Appendix A. Our calculation, based on the theory of Fisher-Hartwig singularities [34,35], not only reproduces the standard bosonization approach [15] but also allows us to compute the numerical prefactor that in general is not possible to obtain. The density matrix reads

$$\rho_2(x,u;y,w) = \frac{2N}{L^2}\rho_\infty^2|e^{i\theta_w} - e^{i\theta_u}|^{-1/2}|e^{i\theta_w} - e^{i\theta_x}|^{-1/2} \times |e^{i\theta_w} - e^{i\theta_y}|^{1/2}|e^{i\theta_y} - e^{i\theta_u}|^{-1/2} \times |e^{i\theta_y} - e^{i\theta_x}|^{-1/2}|e^{i\theta_u} - e^{i\theta_x}|^{1/2}, \quad (11)$$

with $\rho_\infty = G(3/2)^4/\sqrt{2}$ and G is the Barnes function [36]. In addition, if all distances are also much shorter than L we obtain an expression that only depends on terms like $|u-w|$, which is given in Appendix A.

Having determined the two-body density matrix for distances longer than ξ, we need to assess the behavior of $\langle N_p^2\rangle$ and $\langle N_pN_q\rangle$. We start with the former case and notice that, due to the oscillatory behavior of the integrand, the integral is dominated by contributions where $p(y-x)/\hbar$ and $p(w-u)/\hbar$ (direct term) or $p(y-u)/\hbar$ and $p(w-x)/\hbar$ (exchange term) are smaller than or of order 1. We therefore consider configurations in real space where pairs of coordinates are separated by a distance of order $\hbar/p$. By analogy with classical electrodynamics, or to use more sophisticated language, in the Coulomb gas formulation of the Tonks-Girardeau gas [37], we call these pairs dipoles. Moreover, in the thermodynamic limit, it is very unlikely that two dipoles overlap since their size is typically of order $\hbar/p \ll L$. It is then reasonable to assume that the dipoles are well separated and to simplify the expression of the two-body density matrix to $\rho_2(x,u;y,w) \simeq \frac{2N}{L^2}\rho_\infty^2|e^{i\theta_w} - e^{i\theta_u}|^{-1/2}|e^{i\theta_y} - e^{i\theta_x}|^{-1/2}$ in the direct term and a similar expression for the exchange term. In the approximation of the dilute gas of dipoles, the direct and the exchange terms give the same contribution and Eq. (9) factorizes to

$$\langle N_p^2\rangle = \frac{2N}{L^2}\rho_\infty^2\int_0^L \frac{e^{i(p/\hbar)(y-x)}}{\sqrt{\left|\sin\left(\frac{\pi(y-x)}{L}\right)\right|}}d(y-x) \times \int_0^L \frac{e^{i(p/\hbar)(w-u)}}{\sqrt{\left|\sin\left(\frac{\pi(w-u)}{L}\right)\right|}}d(w-u). \quad (12)$$

Here we recognize twice the square of the momentum distribution [see Eq. (34) of Ref. [30] for instance] in the low-momentum limit $\langle N_p\rangle = \frac{\sqrt{N}}{L}\rho_\infty\int_0^L|\sin(\pi x/L)|^{-1/2}dx$. This completes the proof of $\langle N_p^2\rangle = 2\langle N_p\rangle^2$. Note that corrections to this approximation can be calculated by taking into account interactions between dipoles. This can be done by expanding [in Eq. (A7)] $\sqrt{|u-x||w-y|}/\sqrt{|w-x||y-u|} \simeq 1 + (w-u)(y-x)/(u-x)^2$ in the direct term (the

calculation is similar for the exchange term), but this yields positive corrections of the form $\langle N_p\rangle^2/p$, which are subdominant since $\hbar/L \ll p \ll p_F$ in the thermodynamic limit.

We now compute the covariance $\langle N_p N_q\rangle$ using the same procedure. The direct term gives obviously $\langle N_p\rangle\langle N_q\rangle$, whereas the exchange term is a bit more subtle to analyze and reads

$$\langle N_p N_q\rangle_{\rm ex} = \int e^{i(p/\hbar)(y-u)} e^{i(p/\hbar)(w-x)} e^{i[(p-q)/\hbar](u-w)} \times \rho_2(x,u;y,w)dx\,dy\,du\,dw.$$

Using the same arguments as before, the two-body density matrix factorizes and no longer depends on $u-w$, which, due to the presence of the third exponential factor, yields a factor $\delta(p-q)$ in the thermodynamic limit. It is therefore equal to zero for $p \neq q$. Putting pieces together we prove Eq. (10), which suggests that N_p is distributed exponentially. Indeed, putting forth the dilute gas of dipoles approach, we obtain, for all integers n, $\langle N_p^n\rangle = n!\langle N_p\rangle^n$, which is the signature of an exponential distribution

$$P(N_p) = \exp(-N_p/\langle N_p\rangle)/\langle N_p\rangle. \tag{13}$$

This is precisely the result obtained in [15] using bosonization. However, we will show in the next section that this result is also valid beyond the hydrodynamic regime.

IV. SHORT-WAVELENGTH FLUCTUATIONS

We now turn to the regime of high momentum $p \gg p_F$ and extend the previously known results (10) and (13). In other words, we demonstrate that N_p is also exponentially distributed with no correlations in the high-momentum regime. To prove this, we study the behavior of $\rho_2(x,u;y,w)$ for small $|y-x|$ and $|w-u|$ similar to the short-distance expansion of the one-body density-matrix expansion $\rho_1(x) = \rho_1(0) + ax^2 + b|x|^3 + \cdots$ [8,38,39]. We recall that in the case of the average momentum distribution $\langle N_p\rangle$, the leading term giving the so-called p^{-4} contribution comes from the Fourier transform of $|x|^3$. Indeed, the first two contributions give zero for symmetry reasons and the remaining terms are subdominant in the high-p regime. This comes from Watson's lemma [40], which states that if a function $f(z)$ behaves as $|z-a|^\alpha$ in the vicinity of a, then for high p, to leading order in p, $\int_{-\infty}^{+\infty} e^{ipz} f(z-a)dz = 2f(a)e^{ipa}\Gamma(\alpha+1)\cos[\frac{\pi}{2}(\alpha+1)]p^{-(\alpha+1)}$. We will see that the situation is similar for the second moment of the distribution.

Although it is technically possible to perform a cumulant expansion of $\det(\Gamma_n)$, we will not pursue this route. We rather use the development by Lenard [8]. This formal series is an expansion of the two-body bosonic density matrix in terms of the fermionic ones and reads

$$\rho_2(x,u;y,w) = \mathrm{sgn}(u-x)\mathrm{sgn}(w-y)\Bigg(\langle x,u|\rho_F|y,w\rangle + \frac{(-2)}{1!}\int_J \langle x,u,x_3|\rho_F|y,w,x_3\rangle dx_3 + \cdots + \frac{(-2)^n}{n!}\int_J\int_J\cdots\int_J dx_3\cdots dx_{n+2}\langle x,u,x_3,\ldots,x_{n+2}|\rho_F|y,w,x_3,\ldots,x_{n+2}\rangle + \cdots\Bigg), \tag{14}$$

where the interval J is defined as $J \equiv [x,y]\cup[u,w]$ and ρ_F is the fermionic density matrix. The m-body fermionic density matrix reads

$$\langle x,u,x_3,\ldots,x_m|\rho_F|y,w,x_3,\ldots,x_m\rangle = L^{-m}\begin{vmatrix} f(y-x) & f(w-x) & f(x_3-x) & \cdots & f(x_m-x) \\ f(y-u) & f(w-u) & f(x_3-u) & \cdots & f(x_m-u) \\ f(y-x_3) & f(w-x_3) & f(x_3-x_3) & \cdots & f(x_m-x_3) \\ \vdots & \cdots & \cdots & \cdots & \\ f(y-x_m) & f(w-x_m) & f(x_3-x_m) & \cdots & N \end{vmatrix}, \tag{15}$$

with $f(z) \equiv \frac{\sin(N\pi z/L)}{\sin(\pi z/L)}$ for $z \neq 0$ and $f(0) = N$. Although it is possible to compute all terms for finite N, we directly take the thermodynamic limit for the sake of simplicity. Moreover, it is again sufficient to consider dilute dipole configurations since clusters of more than two points give subdominant contributions. This time, it is simply related to the fact that the density matrix vanishes as a power law when two spatial coordinates approach each other (in the Coulomb gas formulation of the Tonks-Girardeau gas, these configurations are strongly penalized by Coulomb repulsion). This can be easily understood by looking at the functional dependence of the many-body wave function (5). In this limit, we have computed this expansion explicitly up to seventh order in $|u-x|$ and $|w-y|$ as it was necessary to obtain the relevant contribution. All the terms are collected in Appendix B.

In order to compute the variance and the correlations, we use a similar dipole decomposition of the Fourier transform with a direct term corresponding to $|x-y| \ll \xi$ and $|w-u| \ll \xi$ with $|u-x| \gg \xi$ and an exchange term with $|x-w| \ll \xi$ and $|y-u| \ll \xi$, also with $|u-x| \gg \xi$. It turns out that, as long as $|u-x| \gg \xi$, the expansion is independent of $u-x$, which makes the calculation of the Fourier transform rather easy. The expansion for the direct term is of the form

$$\rho_2(x,u;y,w) = \sum_{n=0}^{\infty}\sum_{m=0}^{n} A_{m,n}\left|\frac{y-x}{\xi}\right|^m\left|\frac{w-u}{\xi}\right|^{n-m}. \tag{16}$$

When looking carefully at the different terms, it turns out that the relevant term is $A_{3,6}|(y-x)/\xi|^3|(w-u)/\xi|^3$. Performing the same expansion for the exchange term and lumping the two expansions together yields immediately $\langle N_p^2\rangle = 2\langle N_p\rangle^2$,

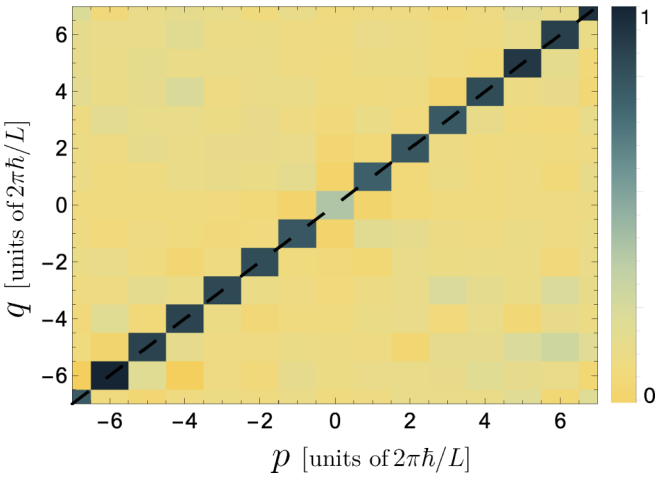

FIG. 3. Normalized correlations between different momentum occupation numbers $\langle N_p N_q\rangle/\langle N_p\rangle\langle N_q\rangle - 1$ for $N = 100$ bosons as a function of p and q. The dashed line indicates the diagonal $p = q$. A cut along the diagonal is visible in the inset of Fig. 2.

with $\langle N_p\rangle = Cp^{-4}$ and $C = \frac{4}{3\pi^2}p_F^4$ since the direct and the exchange contributions are identical. However, for the correlations, the exchange contribution vanishes for the same reason as in Sec. III. Therefore, we also find that no correlation exists between different momenta in this limit. In particular, N_p and N_{-p} are not correlated, as opposed to what happens in the weakly interacting regime [27].

The above analytical part of the calculation can be generalized to the n-body density matrix $\rho_n(z_1, z_2, \ldots, z_n; s_1, s_2, \ldots, s_n)$. This gives access to the nth moment of N_p, $\langle N_p^n\rangle$, resulting in $\langle N_p^n\rangle = n!(\frac{C}{p^4})^n$, in the limit $p \gg p_F$. The knowledge of all the integer moments $\langle N_p^n\rangle$ enables [41,42] us to reconstruct the probability distribution $P(N_p)$, which is therefore exponential.

V. INTERMEDIATE REGIME

We have now proven that the occupation number of a state with momentum p is exponentially distributed according to Eq. (13) and that occupation numbers with a different momentum are uncorrelated for low but nonzero ($\hbar/L \ll p \ll p_F$) and high momenta ($p \gg p_F$). It is then natural to wonder if this statement is correct for intermediate momentum. In that case, we have computed numerically the variance and covariance of N_p using Eqs. (6) and (9). Our results are presented in Figs. 2 and 3 for the standard deviation $\Delta N_p = \sqrt{\langle N_p^2\rangle - \langle N_p\rangle^2}$ and the normalized correlations $\langle N_p N_q\rangle/\langle N_p\rangle\langle N_p\rangle - 1$, respectively.

As can be seen in Fig. 2, the numerically obtained curves ΔN_p and $\langle N_p\rangle$ are almost indistinguishable from each other for all values of p/p_F, not only in the high- and low-momentum regimes. The inset in Fig. 2 shows deviations from this law, which will be discussed in the next section. Although it is not a proof, it is strong evidence that the equation $\langle N_p^2\rangle = 2\langle N_p\rangle^2$ is valid for any momentum p, as long as p is not too close to zero, as discussed in Sec. VI below. It is therefore reasonable to believe that N_p is distributed exponentially for any value of $p \neq 0$. This has the important consequence that for a Tonks-Girardeau gas, the relative fluctuations of N_p never vanish in the thermodynamic limit. They are always equal to the signal itself. This is schematized in Fig. 1.

Concerning the correlations, one can also observe in Fig. 3 that they exist only for $p = q$, in agreement with Eq. (10). Indeed, only one straight line on the colormap $\langle N_p N_q\rangle/\langle N_p\rangle\langle N_q\rangle - 1$ as a function of p and q is visible, the rest of the colormap being zero. This is in sharp contrast to the physics of a weakly interacting Bose gas discussed in Refs. [11,13,14], where, for instance, correlations between p and $-p$ are clearly visible. This is not really a surprise since these pair correlations stem from the existence of a condensate and are the hallmark of long-range coherence. They basically emerge from the low-energy excitations of this system that are phonons which are quasiparticles with equal weight of opposite momentum components, whereas in the Tonks-Girardeau gas, the low-energy excitations are particle-hole-like and independent of each other.

VI. QUASICONDENSATE MODE

So far, we have focused on the statistical distribution and correlations of momentum state occupation numbers with nonzero momentum. As discussed in [15], the quasicondensate mode which has zero momentum must be treated differently. Using arguments based on Bogoliubov theory in the weak-coupling regime, Lovas *et al.* explained that the distribution of N_0 was of Gumbel type.[1] However, at larger coupling (when the Luttinger parameter K approaches one in Fig. 3 of [15]), important deviations from this prediction are visible. In the following, we briefly discuss how this problem is related to other models that have been studied in the literature and discuss some important results such as the variance and the shape of the distribution of N_0.

The nth moment of the number of bosons in the zero-momentum state $\langle N_0^n\rangle$ is given by the formula

$$\frac{\langle N_0^n\rangle}{(\rho_\infty\sqrt{2N})^n} = \int_0^{2\pi}\cdots\int_0^{2\pi}\prod_{1\leqslant i<j\leqslant n}\left|4\sin\left(\frac{\theta_i-\theta_j}{2}\right)\sin\left(\frac{\theta_i'-\theta_j'}{2}\right)\right|^\alpha\left[\prod_{i=1}^n\prod_{j=1}^n\left|2\sin\left(\frac{\theta_i-\theta_j'}{2}\right)\right|^\alpha\right]^{-1}\frac{d\theta_1}{2\pi}\cdots\frac{d\theta_n}{2\pi}\frac{d\theta_1'}{2\pi}\cdots\frac{d\theta_n'}{2\pi}, \tag{17}$$

[1] In the weak-interaction regime [15], $x = (N_0 - \langle N_0\rangle)/\Delta N_0$ (where ΔN_0 is the standard deviation of N_0) is distributed according to the Gumbel distribution $P(x) = c\exp[cx - \gamma - \exp(cx - \gamma)]$, with $c = \pi/\sqrt{6}$ and $\gamma \simeq 0.5772$ Euler's constant.

with $\alpha = 1/2$. This kind of expression shows up in other physical problems and has been studied in different contexts. For instance, if divided by $n!$[2], it can be interpreted as the canonical partition function of a neutral two-component Coulomb gas with $2n$ (in total) logarithmically interacting charges [43]. Then θ_i and θ'_j are the positions of the positive and negative charges on the unit circle, respectively. The inverse temperature of the Coulomb gas is $\beta = \alpha$. It is also related to the partition function which describes tunneling through a barrier of an interacting spinless Luttinger liquid with attractive interactions [44] and the interaction parameter $g = 4$ in the notation of Ref. [44]. The gas is in the disordered phase, at a temperature T well above the Kosterlitz-Thouless transition $T_{\rm KT}$, which occurs at $\beta = 1/T_{\rm KT} = 2$ in their units. Finally, this problem of finding the full distribution of N_0 is closely related to the full counting statistics of the average interference patterns between two Bose condensates [45,46]. However, in the case of Refs. [45,46], there are two condensates, each one having a Luttinger parameter K. Consequently, Eq. (17), giving $\langle N_0^n \rangle$, translates to the same problem they studied but with $\alpha = \frac{1}{2K}$ and not $1/K$. For the Tonks-Girardeau gas, $\alpha = 1/2$ and we can thus use the results derived in Ref. [45], with $K = 2$, instead of $K = 1$, as one might naively think. Therefore, most of the results about the distribution of N_0 are available in the references mentioned above. In particular, using previous work by Bazhanov *et al.* [47], the authors of Ref. [45] were able to obtain a distribution related to $P(N_0)$ exactly.

We now discuss several simple results, namely, the two first moments of the distribution and its shape. The average value of N_0 was calculated in [30] and reads

$$\langle N_0 \rangle = \frac{\sqrt{2\pi}}{[\Gamma(3/4)]^2} \rho_\infty \sqrt{N}, \tag{18}$$

while the second moment can be evaluated numerically from Eq. (17) and gives[2]

$$\langle N_0^2 \rangle \simeq 1.33 \langle N_0 \rangle^2, \tag{19}$$

which shows that N_0 is no longer exponentially distributed: $\langle N_0^2 \rangle \neq 2\langle N_0 \rangle^2$. Nevertheless, the fluctuations of N_0 are proportional to its average and therefore do not disappear in the thermodynamic limit either as it has also been noticed in lattice systems [12]. The prefactor in Eq. (19) is smaller than 2, which means that fluctuations are smaller in the quasicondensate than in other modes. We associate this with a reminiscent effect of coherence that would reduce fluctuations in the condensate. This result is depicted in the inset of Fig. 2. At $p = 0$ it can be seen that the prediction of Eq. (19) is verified (see the lower black horizontal line) and that for $p \neq 0$ the statistics quickly converge to the exponential one.

In addition to the average and the variance, we have access to the full distribution. Following the method employed in Ref. [45] (see Appendix C) for $K = 2$ in the notation therein,

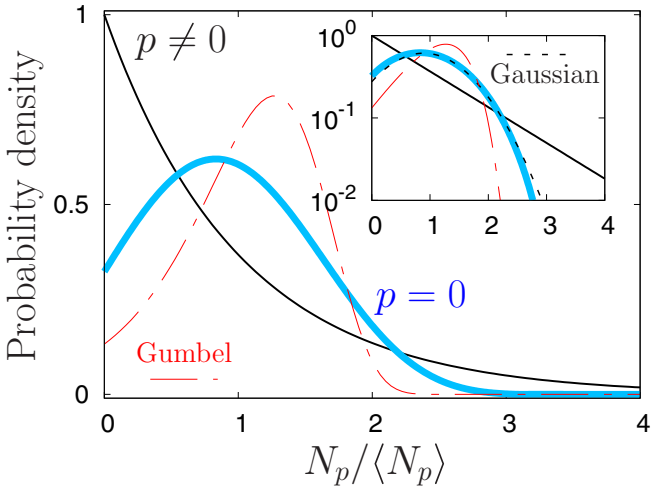

FIG. 4. Probability densities of $N_0/\langle N_0 \rangle$ (thick blue line) and $N_p/\langle N_p \rangle$ (thin black line) for $p \neq 0$ (but $p \gg \hbar/L$). The inset shows the same data in semilogarithmic scale. The red dot-dashed curve is the Gumbel distribution (see footnote 1) and the black dashed curve is a Gaussian fit for guidance.

we have calculated the distribution of N_0. The result is shown in Fig. 4 and demonstrates that in the Tonks-Girardeau regime, it is neither exponential nor Gumbel but still contains large fluctuations. Some insight into the full distribution of N_0 can also be obtained by looking at the asymptotic behavior of the moments. Using the results of Ref. [37], we obtain, for $n \gg 1$,

$$\langle N_0^n \rangle \simeq (\rho_\infty \sqrt{2N})^n \exp\left[\tfrac{1}{2} n \ln n + O(n)\right], \tag{20}$$

which can easily be checked to be the asymptotic expression of the moments of a positive Gaussian-distributed random variable. This is indeed what is apparent in the inset of Fig. 4, where we show the probability density in logarithmic scale. This result can also be retrieved analytically by looking at the behavior of spectral determinants, along the lines of Refs. [45,46] (see Appendix C). The advantage of this method is that it also permits us to obtain information on the behavior of $P(N_p)$ for very low but nonzero momenta p, but we leave this for future investigation.

VII. CONCLUSION AND PERSPECTIVES

In this work we have proposed a scheme to compute the quantum fluctuations, at zero temperature, of the number of particles N_p with momentum p, for the Tonks-Girardeau gas. We have shown analytically in the low- ($\hbar/L \ll p \ll p_F$) and high-momentum limits ($p \gg p_F$) and have given strong numerical evidence for intermediate values of momentum that N_p is distributed according to an exponential law. In particular, we have demonstrated that the standard deviation of the momentum distribution was equal to its mean value. In addition, we have computed the covariance $\langle N_p N_q \rangle$ and shown that correlations were only visible on the axis $p = q$ and that correlations between N_p and N_{-p} were suppressed, contrary to the case of a weakly interacting Bose gas described by Bogoliubov quasiparticles. Finally, the distribution of the quasicondensate mode at $p = 0$ was shown to behave differently, as already observed for weak and moderate interactions

[2]The multidimensional integral in Eq. (17) with $n = 2$ has been evaluated with a Monte Carlo algorithm with 10^8 points. The statistical sampling over 10 000 configurations gives $\langle N_0^2 \rangle / \langle N_0 \rangle^2 = 1.328$ with a standard deviation equal to 0.015.

in [15]. We argued that, in the Tonks regime, the tail of its distribution is neither exponential nor Gumbel but rather of Gaussian type. The case of correlations for very low but nonzero momentum ($p \simeq \hbar/L$) is more difficult and is left for future investigation.

Our findings can be relevant for ultracold-atom experiments where high-order correlation functions in momentum space can be measured, for instance, with time-of-flight techniques [48]. In actual experiments, atoms are generally released from a harmonic trap and the effect of the well potential on the momentum distribution has to be taken into account [48,49]. Inclusion of finite temperature would also be a natural generalization of this work [50–52] as well as finite interaction corrections in the regime of high momentum [53]. Investigating the weak coupling or intermediate coupling of the boson interaction, i.e., using the Lieb-Liniger model [28], would also provide more insight [54–56] into how the quasicondensate correlations build up [57]. Finally, another important lead to follow would be the study of the fermionic counterpart where generalization of random matrix theories [58,59], including off-diagonal contributions of the density matrix, would be considered.

ACKNOWLEDGMENTS

We would like to acknowledge helpful discussions with D. Clément, J. Decamp, and M. Rigol. The work of D.C. was supported by the Swiss National Science Foundation and NCCR QSIT.

APPENDIX A: ASYMPTOTIC BEHAVIOR OF THE TWO-PARTICLE DENSITY MATRIX FROM DETERMINANTS WITH FISHER-HARTWIG SINGULARITIES

In this Appendix we derive the expression of the two-body density matrix of the Tonks-Girardeau gas in terms of Toeplitz matrices and compute its long-distance approximation using asymptotic properties of these matrices [34,35].

Starting from Eq. (4), inserting the ground-state wave function (5), and defining $\theta_{x_i} = 2\pi x_i/L$, we obtain $\rho_2(x, u; y, w)$,

$$\rho_2 = \frac{1}{N!L^N}\int_0^{2\pi}\cdots\int_0^{2\pi}|e^{i\theta_x}-e^{i\theta_u}||e^{i\theta_w}-e^{i\theta_y}| \times\left(\prod_{l=3}^{N}|e^{i\theta_x}-e^{i\theta_l}||e^{i\theta_y}-e^{i\theta_l}||e^{i\theta_u}-e^{i\theta_l}||e^{i\theta_w}-e^{i\theta_l}|\right) \times\prod_{3\leqslant m<n\leqslant N}|e^{i\theta_m}-e^{i\theta_n}|^2 dx_3\cdots dx_N. \tag{A1}$$

Then using the formulation in terms of a determinant of a Toeplitz matrix (see Refs. [8,60]), we use the lemma

$$\frac{1}{N!}\int_0^{2\pi}\cdots\int_0^{2\pi}\prod_{l=1}^{N}f(\theta_l)\prod_{1\leqslant n<m\leqslant N}|e^{i\theta_m}-e^{i\theta_n}|^2\frac{d\theta_1}{2\pi}\cdots\frac{d\theta_N}{2\pi} = \det(M), \tag{A2}$$

where M is the square matrix with elements $M_{m,n} = \int_0^{2\pi} e^{i\theta(m-n)}f(\theta)\frac{d\theta}{2\pi}$. This lemma follows directly from expressing $\prod_{3\leqslant m<n\leqslant N}|e^{i\theta_m}-e^{i\theta_n}|^2$ as the square of a Vandermonde determinant, namely,

$$\prod_{1\leqslant n<m\leqslant N}|e^{i\theta_m}-e^{i\theta_n}|^2 = \sum_{\mathcal{P},\mathcal{Q}}\epsilon(\mathcal{P})\epsilon(\mathcal{Q})\prod_{l=1}^{N}e^{i\theta_l[\mathcal{P}(l)-\mathcal{Q}(l)]}, \tag{A3}$$

where $\mathcal{P}$ and $\mathcal{Q}$ are permutations of the N integers from 1 to N and $\epsilon(\mathcal{P})$ is the signature of the permutation $\mathcal{P}$. The sum on $\mathcal{P}$ runs over all the $N!$ permutations, as does the one on $\mathcal{Q}$. In our case, we take out the term $\frac{1}{L^N}|e^{i\theta_x}-e^{i\theta_u}||e^{i\theta_w}-e^{i\theta_y}|$ and apply the lemma with $N-2$ instead of N and

$$f(\theta) = |e^{i\theta_x}-e^{i\theta}||e^{i\theta_y}-e^{i\theta}||e^{i\theta_u}-e^{i\theta}||e^{i\theta_w}-e^{i\theta}|. \tag{A4}$$

Since $|e^{i\theta_x}-e^{i\theta}| = 2|\sin(\frac{\theta-\theta_x}{2})|$, we obtain Eqs. (6)–(8).

We now evaluate the large-N behavior of the two-body density matrix. In the spirit of Refs. [61,62], we adapt the method used there for the one-body density matrix to the long-distance behavior of the two-body density matrix which is governed by the Fisher-Hartwig singularities of the matrix $\Gamma_{i,j}$, in Eqs. (6) and (7). We suppose that x, y, u, and w are all separated by a distance longer than L/N. Starting from Eq. (6), we need to evaluate the asymptotic behavior of $\det(\Gamma_{i,j})$ for large N, with θ_x, θ_y, θ_u, and θ_w larger than N^{-1}. The symbol $F(\theta)$ of the Toeplitz matrix $\Gamma_{i,j}$ is given by Eq. (8) and satisfies $\int_0^{2\pi}\ln F(\theta)d\theta = 0$. This implies that the determinant does not increase nor does it decay exponentially for large N. There are however four distinct Fisher-Hartwig singularities located at $\theta = \theta_x, \theta_y, \theta_u$, and θ_w. These singularities are all of the same type, a discontinuity of the slope in $F(\theta)$; in other words, there are four α-type singularities in the notation of Ref. [62], with $\alpha = 1/2$. Applying theorems (2) and (3) from Ref. [62], we obtain

$$\det(\Gamma_{i,j}) \simeq NG(3/2)^8|e^{i\theta_y}-e^{i\theta_x}|^{-1/2}|e^{i\theta_y}-e^{i\theta_u}|^{-1/2} \times|e^{i\theta_w}-e^{i\theta_x}|^{-1/2}|e^{i\theta_w}-e^{i\theta_u}|^{-1/2}|e^{i\theta_w}-e^{i\theta_y}|^{-1/2} \times|e^{i\theta_u}-e^{i\theta_x}|^{-1/2}, \tag{A5}$$

with G the Barnes function [36]. Now, taking into account the prefactor in Eq. (6),

$$\rho_2(x, u; y, w) \simeq (N/L^2)G(3/2)^8|e^{i\theta_y}-e^{i\theta_x}|^{-1/2}|e^{i\theta_y}-e^{i\theta_u}|^{-1/2} \times|e^{i\theta_w}-e^{i\theta_x}|^{-1/2}|e^{i\theta_w}-e^{i\theta_u}|^{-1/2} \times|e^{i\theta_w}-e^{i\theta_y}|^{+1/2}|e^{i\theta_u}-e^{i\theta_x}|^{+1/2}, \tag{A6}$$

which is Eq. (11). In order to retrieve the familiar result of bosonization on the infinite line, we suppose that all arguments x, y, u, w are small with respect to L, but can be large with respect to L/N. This allows us to approximate $|e^{i\theta_y}-e^{i\theta_x}|^{-1/2} \simeq \sqrt{L/2\pi}|y-x|^{-1/2}$ and yields

$$\rho_2(x, u; y, w) = N[G(3/2)^8/2\pi L]|w-u|^{-1/2}|w-x|^{-1/2} \times|w-y|^{1/2}|y-u|^{-1/2}|y-x|^{-1/2}|u-x|^{1/2}. \tag{A7}$$

APPENDIX B: THERMODYNAMIC LIMIT OF $\rho_2(x,u;y,w)$ FOR $|u-x| \gg \xi$ AT SHORT DISTANCES $|y-x|$ AND $|w-u| \ll \xi$

We give here explicit expressions of the Lenard expansion in the thermodynamic limit, in the regime of the dilute gas of dipoles, up to seventh order. These results are simply obtained by computing the determinants in the large-N limit. Here we consider the configuration where x and y and u and w constitute the two dipoles ($|y-x| \ll \xi$ and $|w-u| \ll \xi$) that are far apart ($|u-x| \gg \xi = L/N$), but it is straightforward to obtain all possible permutations since the bosonic density is symmetric with respect to permutations. In that case, an important simplification comes from the fact that $\frac{\sin[\pi N(u-x)/L]}{\sin[\pi(u-x)/L]}$ is always of order 1 and never of order N, giving lower powers of N. A tedious calculation to the seventh order yields

$$\rho_2(x,u;y,w) = \frac{N^2}{L^2}\mathrm{sgn}(u-x)\mathrm{sgn}(w-y)\sum_{n=0}^{7} T_n, \tag{B1}$$

with

$$T_0 = 1, \quad T_1 = 0, \tag{B2}$$

$$T_2 = -\frac{\pi^2}{6}(Y^2+W^2), \quad T_3 = -\frac{\pi^2}{9}(|Y|^3+|W|^3), \tag{B3}$$

$$T_4 = \left(\frac{\pi^4}{120}+\frac{\pi^2}{9}\right)(Y^4+W^4)+\frac{\pi^4}{36}Y^2W^2, \tag{B4}$$

$$T_5 = -\frac{11}{1350}\pi^4(|Y|^5+|Y|^5)-\frac{\pi^4}{54}(|Y|^3W^2+Y^2|W|^3), \tag{B5}$$

$$T_6 = \left(\frac{\pi^2}{9}\right)^2|Y|^3|W|^3-\left(\frac{\pi^6}{5040}+\frac{11}{450}\pi^4\right)(Y^6+W^6) -\left(\frac{\pi^6}{720}+\frac{\pi^4}{54}\right)(Y^4W^2+Y^2W^4), \tag{B6}$$

$$T_7 = \frac{61}{264\,600}\pi^6(|Y|^7+|W|^7)+\frac{11}{1800}\pi^6(|Y|^5W^2+Y^2|W|^5) +\frac{\pi^6}{1080}(Y^4|W|^3+|Y|^3W^4), \tag{B7}$$

where $Y = N(y-x)/L$ and $W = N(w-u)/L$. To obtain Eq. (16) we have defined

$$T_n = \sum_{m=0}^{n} A_{m,n}|Y|^m|W|^{n-m}. \tag{B8}$$

APPENDIX C: DISTRIBUTION OF N_0 FROM SPECTRAL DETERMINANTS

We briefly explain here how we have calculated the distribution of N_0 shown in Fig. 4 and how the Gaussian behavior of the tail of the distribution $P(N_0)$ can be retrieved with the help of spectral determinants of Ref. [47]. Using the formulation of Ref. [45] (for a different problem of interferences between two interacting bosonic gases but mathematically similar to the problem considered in this article), the statistical properties of N_0 are related to the spectrum $\{\varepsilon_n\}$ of the radial sextic oscillator

$$-\frac{d^2\psi(r)}{dr^2}+\left(r^6+\frac{\ell(\ell+1)}{r^2}\right)\psi(r) = \varepsilon_n\psi(r), \tag{C1}$$

with angular momentum $\ell = -\frac{1}{2}$ and $r \in [0,+\infty[$. The distribution of N_0 is given by the integral [45]

$$P(\alpha) = 2\int_0^\infty \prod_{n=1}^{\infty}\left(1-\kappa\frac{x^2}{\varepsilon_n}\right)J_0(2x\sqrt{\alpha})x\,dx, \tag{C2}$$

with $\alpha = N_0/\langle N_0\rangle$, $\kappa = 8\sqrt{2}\Gamma(3/4)^2/\pi^2$, and J_0 the Bessel function. This is the result shown in Fig. 4.

The moments of the distribution can be cast in the form

$$\langle N_0^n\rangle \equiv (\rho_\infty\sqrt{2N})^n Z_{2n} = (n!)^2(\rho_\infty\sqrt{2N}\kappa)^n \sum_{i_1,i_2,\ldots,i_n,\ \text{all different}} \prod \varepsilon_{i_1}^{-1}\varepsilon_{i_2}^{-1}\cdots\varepsilon_{i_n}^{-1}. \tag{C3}$$

As explained in Ref. [47], for j larger than 2 basically, ε_j increases as $j^{3/2}$ and thus Z_{2n} behaves as $\sqrt{n!}$ for large n. This in turn implies that $P(N_0) \simeq \exp(-CN_0^2)$ for large N_0, where C is a real positive constant. The behavior of $\langle N_p^n\rangle$ for low but nonzero $p = j\frac{2\pi\hbar}{L}$ is obtained in the same way, except that now the energy levels ε_i are no longer the energy levels of the oscillator in (C2) with $l = -\frac{1}{2}$ but with $l = 4j-\frac{1}{2}$. For j much smaller than n, the behavior of $\langle N_p^n\rangle$ still has the same behavior as $\langle N_0^n\rangle$, so the tail of the distribution $P(N_p)$ is also Gaussian. However, for n much smaller than j, $\langle N_p^n\rangle$ behaves as $n!\langle N_p\rangle^n$, signaling the exponential behavior of $P(N_p)$ for $N_p \ll j\langle N_p\rangle$.

[1] I. Bloch, J. Dalibard, and W. Zwerger, Rev. Mod. Phys. **80**, 885 (2008).

[2] M. Lewenstein, A. Sanpera, and V. Ahufinger, *Ultracold Atoms in Optical Lattices: Simulating Quantum Many Body Physics* (Oxford University Press, Oxford, 2012).

[3] M. A. Cazalilla, R. Citro, T. Giamarchi, E. Orignac, and M. Rigol, Rev. Mod. Phys. **83**, 1405 (2011).

[4] X. W. Guan, M. T. Batchelor, and C. Lee, Rev. Mod. Phys. **85**, 1633 (2013).

[5] E. Altman, E. Demler, and M. D. Lukin, Phys. Rev. A **70**, 013603 (2004).

[6] M. Girardeau, J. Math. Phys. **1**, 516 (1960).

[7] V. E. Korepin, N. M. Bogoliubov, and A. G. Izergin, *Quantum Inverse Scattering Method and Correlation Functions* (Cambridge University Press, Cambridge, 1983).

[8] A. Lenard, J. Math. Phys. **5**, 930 (1964); **7**, 1268 (1966).

[9] A. J. Leggett, *Quantum Liquids: Bose Condensation and Cooper Pairing in Condensed-Matter Systems* (Oxford University Press, Oxford, 2006).

[10] J. Decamp, J. Jünemann, M. Albert, M. Rizzi, A. Minguzzi, and P. Vignolo, Phys. Rev. A **94**, 053614 (2016).

[11] L. Mathey, A. Vishwanath, and E. Altman, Phys. Rev. A **79**, 013609 (2009).

[12] K. He and M. Rigol, Phys. Rev. A **83**, 023611 (2011).

[13] B. Fang, A. Johnson, T. Roscilde, and I. Bouchoule, Phys. Rev. Lett. **116**, 050402 (2016).

[14] I. Bouchoule, M. Arzamasovs, K. V. Kheruntsyan, and D. M. Gangardt, Phys. Rev. A **86**, 033626 (2012).

[15] I. Lovas, B. Dóra, E. Demler, and G. Zaránd, Phys. Rev. A **95**, 053621 (2017).

[16] I. Lovas, B. Dóra, E. Demler, and G. Zaránd, Phys. Rev. A **95**, 023625 (2017).

[17] J. Dobrzyniecki and T. Sowiński, Phys. Rev. A **99**, 063608 (2019).

[18] C. Carcy, H. Cayla, A. Tenart, A. Aspect, M. Mancini, and D. Clément, Phys. Rev. X **9**, 041028 (2019).

[19] J.-C. Jaskula, G. B. Partridge, M. Bonneau, R. Lopes, J. Ruaudel, D. Boiron, and C. I. Westbrook, Phys. Rev. Lett. **109**, 220401 (2012).

[20] W. G. Unruh, Phys. Rev. Lett. **46**, 1351 (1981).

[21] R. Balbinot, A. Fabbri, S. Fagnocchi, A. Recati, and I. Carusotto, Phys. Rev. A **78**, 021603(R) (2008).

[22] A. Recati, N. Pavloff, and I. Carusotto, Phys. Rev. A **80**, 043603 (2009).

[23] A. Fabbri and N. Pavloff, SciPost Phys. **4**, 019 (2018).

[24] J. Ramón Muñoz de Nova, K. Golubkov, V. I. Kolobov, and J. Steinhauer, Nature (London) **569**, 688 (2019).

[25] T. Giamarchi, *Quantum Physics in One Dimension* (Clarendon, Oxford, 2004).

[26] J. van Delft and H. Schoeller, Ann. Phys. (Leipzig) **7**, 225 (1998).

[27] N. M. Bogoliubov and D. V. Shirkov, *Introduction to the Theory of Quantized Fields* (Wiley, New York, 1980).

[28] E. H. Lieb and W. Liniger, Phys. Rev. **130**, 1605 (1963).

[29] M. Olshanii, Phys. Rev. Lett. **81**, 938 (1998).

[30] P. J. Forrester, N. E. Frankel, T. M. Garoni, and N. S. Witte, Phys. Rev. A **67**, 043607 (2003).

[31] S. Tan, Ann. Phys. (NY) **323**, 2952 (2008); **323**, 2971 (2008); **323**, 2987 (2008).

[32] R. J. Wild, P. Makotyn, J. M. Pino, E. A. Cornell, and D. S. Jin, Phys. Rev. Lett. **108**, 145305 (2012).

[33] H. Ott, Rep. Prog. Phys. **79**, 054401 (2016).

[34] T. Ehrhardt, Oper. Theory Adv. Appl. **124**, 217 (2001).

[35] P. Deift, A. Its, and I. Krasovsky, Ann. Math. **174**, 1243 (2011).

[36] L. Gradshteyn and I. Ryzhik, *Table of Integrals, Series, and Products* (Elsevier, Amsterdam, 1996).

[37] P. Fendley, F. Lesage, and H. Saleur, J. Stat. Phys. **79**, 799 (1995).

[38] H. G. Vaidya and C. A. Tracy, J. Math. Phys. **20**, 2291 (1979).

[39] A. Minguzzi, P. Vignolo, and A. Tosi, Phys. Lett. A **294**, 22 (2002).

[40] M. J. Lighthill, *Introduction to Fourier Analysis and Generalized Functions* (Cambridge University Press, Cambridge, 1959).

[41] N. I. Akhiezer, *The Classical Moment Problem* (Oliver and Boyd, Edinburgh, 1963).

[42] B. Simon, Adv. Math. **137**, 82 (1998).

[43] L. Samaj, J. Stat. Phys. **152**, 599 (2013).

[44] C. L. Kane and M. P. A. Fisher, Phys. Rev. B **46**, 15233 (1992).

[45] V. Gritsev, E. Altman, E. Demler, and A. Polkovnikov, Nat. Phys. **2**, 705 (2006).

[46] S. Hofferberth, I. Lesanovsky, T. Schumm, A. Imambekov, V. Gritsev, E. Demler, and J. Schmiedmayer, Nat. Phys. **4**, 489 (2008); V. Gritsev, A. Polkovnikov, and E. Demler, Phys. Rev. B **75**, 174511 (2007).

[47] V. V. Bazhanov, S. L. Lukyanov, and A. B. Zamolodchikov, J. Stat. Phys. **102**, 567 (2001); Commun. Math. Phys. **177**, 381 (1996); **190**, 247 (1997); **200**, 297 (1999); Nucl. Phys. B **549**, 529 (1999).

[48] R. Chang, Q. Bouton, H. Cayla, C. Qu, A. Aspect, C. I. Westbrook, and D. Clément, Phys. Rev. Lett. **117**, 235303 (2016).

[49] H. Yao, D. Clément, A. Minguzzi, P. Vignolo, and L. Sanchez-Palencia, Phys. Rev. Lett. **121**, 220402 (2018).

[50] P. Vignolo and A. Minguzzi, Phys. Rev. Lett. **110**, 020403 (2013).

[51] P. Deuar, A. G. Sykes, D. M. Gangardt, M. J. Davis, P. D. Drummond, and K. V. Kheruntsyan, Phys. Rev. A **79**, 043619 (2009).

[52] W. Xu and M. Rigol, Phys. Rev. A **92**, 063623 (2015).

[53] G. Lang, P. Vignolo, and A. Minguzzi, Eur. Phys. J.: Spec. Top. **226**, 1583 (2017).

[54] D. M. Gangardt and G. V. Shlyapnikov, Phys. Rev. Lett. **90**, 010401 (2003).

[55] D. M. Gangardt and G. V. Shlyapnikov, New J. Phys. **5**, 79 (2003).

[56] M. Olshanii and V. Dunjko, Phys. Rev. Lett. **91**, 090401 (2003).

[57] E. J. K. P. Nandani, R. A. Römer, S. Tan, and X. W. Guan, New J. Phys. **18**, 055014 (2016).

[58] B. Sutherland, J. Math. Phys. **12**, 246 (1971).

[59] D. S. Dean, P. Le Doussal, S. N. Majumdar, and G. Schehr, J. Phys. A: Math. Theor. **52**, 144006 (2019).

[60] U. Grenander and G. Szegö, *Toeplitz Form and their Applications* (University of California Press, Berkeley, 1958).

[61] A. Lenard, Pacific J. Math. **42**, 137 (1972).

[62] E. L. Basor and C. A. Tracy, Physica A **177**, 167 (1991).